Zener tunneling effect of excitons in shallow superlattices

S. Glutsch and F. Bechstedt
Friedrich-Schiller-Universität Jena, Institut für Festkörpertheorie und Theoretische Optik, Max-Wien-Platz 1, 07743 Jena, Germany

B. Rosam and K. Leo
Technische Universität Dresden, Institut für Angewandte Photophysik, 01062 Dresden, Germany

(Received 28 August 2000; published 1 February 2001)

The Zener effect in the optical absorption of shallow superlattices is studied theoretically and experimentally. The comparison between the Kane approximation, which is the widely accepted picture so far, and a numerical calculation including all subbands, provides clear evidence for the Zener effect. The experimental spectra are in good agreement with the theory. The measured line broadening as a function of the electric field behaves as predicted by the Zener theory, and is of the same order of magnitude as calculated from the sample parameters. We also suggest absorption measurements in a magnetic field in growth direction, which would provide an even clearer demonstration for the transition between discrete transitions and the continuum due to Zener tunneling.

DOI: 10.1103/PhysRevB.63.085307 PACS number(s): 78.20.Jq, 71.35.−y, 78.66.Fd

I. INTRODUCTION

The electronic structure of a periodic potential under a static electric field is of high interest due to its importance for carrier transport in solids. Key theoretical contributions were already made at the beginning of last century by Bloch and Zener. Of particular interest are effects at high static field, leading to oscillatory motion due to Bragg reflections of electrons at the lattice (Bloch oscillations) and to the transfer of electrons to higher bands (Zener breakdown). A detailed experimental investigation of these effects based on bulk solids was not possible since their observation requires extremely high fields (typically MV/cm) and is often masked by other effects.

However, there were long-standing theoretical debates about the electronic structure of periodic potentials with static field. It was already mentioned in Wannier's original paper that the energy spectrum should be continuous.[1] Nevertheless, various authors claimed that there should be ladders of discrete states. In 1977, Avron and co-workers proved analytically that the spectrum is absolutely continuous.[2]

The experimental situation was decisively changed by the introduction of the semiconductor superlattice.[3] In these systems, the bandwidths are rather small, requiring only comparatively low fields to observe the above-mentioned effects. The electronic structure of semiconductor superlattices can be adjusted over a wide range to achieve the desired properties. Linear absorption measurements yielded the observation of the Wannier-Stark ladder in these systems. Bloch oscillations have also been investigated in detail in semiconductor superlattices.

Traditionally, these experiments have been described in terms of Wannier-Stark ladders. It was shown that the Wannier-Stark ladder picture suffices to explain absorption measurements[4–8] as well as nonlinear optical experiments.[9,10] For high electric fields, Zener tunneling is expected to take place. Signatures of Zener tunneling have been reported in recent years.[11–13] These papers mainly focus on the coupling of a finite number of minibands, also known as resonant Zener tunneling. A recent theoretical analysis predicts a sharp decrease of the lifetime of Wannier-Stark states for level crossings between different Wannier-Stark ladders.[14]

In the original paper, the Zener effect describes an open system with tunneling between one band and the continuum of all other bands under the influence of an electric field F.[15,16] The tunneling rate γ for interminiband transitions is equal to

$$\gamma = \frac{e|F|a}{2\pi\hbar} \exp\left[-\frac{m_e a (\Delta E)^2}{4\hbar^2 e|F|} \right], \tag{1}$$

where m_e is the effective electron mass, a is the superlattice period, and ΔE is the gap between the first and second miniband. This result was derived for nearly-free electrons, under the assumption that the other gaps are significantly smaller than ΔE. Thus tunneling is considered between the first miniband and the bulk of all other minibands. The quantity $\hbar\gamma$ can be considered as the imaginary part of the eigenvalues, which leads to an exponential decrease of the wave function and to a broadening in the optical spectrum.

In order to detect Zener tunneling in the optical absorption, $\hbar\gamma$ needs to be larger than or equal to the homogeneous line broadening $\hbar\epsilon$, which results from electron-phonon interaction. Furthermore, without magnetic field, $\hbar\gamma$ should exceed the natural linewidth of the Fano resonances. This nonresonant Zener tunneling has been observed in the optical absorption of strongly coupled superlattices,[17] and has been explained mainly in term of interaction-free electrons and holes.[18]

A major complication in the theoretical modeling is the fact that the optical absorption near the band gap, as well as the nonlinear optical properties, are dominated by excitons. The absorption spectrum, including excitons, is very different from the spectrum calculated with interaction-free electrons and holes. For a quantitative agreement with the experiment it is necessary to include Coulomb interaction.

TABLE I. Material and sample parameters, dimensionless units.

Parameter	Symbol, Formula	Value
Electron effective mass	m_e	$0.0670\,m_0$
Hole perpendicular effective mass[a]	m_{hz}	$0.377\,m_0$
Hole in-plane effective (cyclotron) mass[a]	$m_{h\rho}$	$0.491\,m_0$
Hole spherical (density-of-states) mass	m_{hs}	$0.5\,m_0$
GaAs band gap at 10 K	E_g	1.515 eV
Band discontinuities[b]	H_e	$790\,x$ meV
	H_h	$460\,x$ meV
Static dielectric constant	ε	13.1
Al content	x	8 %
Superlattice period	a	115 Å
Barrier thickness	b	39 Å
Homogeneous broadening	$\hbar\epsilon$	1 meV

[a]Reference 29.
[b]Reference 30.

Especially for shallow superlattices, the calculation of the optical spectrum, including excitons, is a particular challenge. Field-induced broadening of the absorption spectra has been studied in quantum wells with weak and strong confinement a couple of years ago, where the theoretical model was based upon quasi-localized states.[19] Recently, a similar approach was used to calculate optical spectra of shallow superlattices in an electric field.[20] In both cases, the experimentally observed line broadening was reproduced by the numerical calculation.

The Coulomb interaction between excitons and the continuum of different Wannier-Stark states also leads to Fano interference and to a natural linewidth, which overshadows the Zener effect. In order to distinguish between both mechanisms, it is desirable to compare the experimental data with those calculations that include, and those that neglect, Zener tunneling. A magnetic field applied in the growth direction suppresses the Fano effect and the continuum states. Then the in-plane motion is subjected to Landau quantization. A measurement in a magnetic field would provide clear-cut evidence for the Zener effect, because all line broadening results from Zener tunneling.

In this paper, we calculate optical spectra of shallow superlattices in electric fields, including Coulomb interaction. The computational method uses finite differences in real space, does not rely on single-particle eigenstates, and is not limited in the number of minibands. We compare the numerical exact result for the electron-hole Schrödinger equation with calculations including only one pair of minibands. This allows us to clearly distinguish between the effect of Fano interference and Zener tunneling. We also carry out calculations for perpendicular magnetic field, which show a line broadening exclusively on the account of Zener tunneling. Furthermore, we show absorption spectra measured on a shallow superlattice in a perpendicular electric field, which are in good agreement with the theoretical calculations. A fit of the measured linewidth to the Zener tunneling rate further supports the interpretation as Zener tunneling.

The paper is organized as follows. After this introduction, in Sec. II we specify the sample parameters and explain the calculation of the absorption spectra in real space and by expansion into Wannier functions. Some experimental details are given in Sec. III. In Sec. IV, we discuss the numerical results without and with magnetic field, compare experimental and theoretical spectra, and compare the line broadening with the tunneling rate predicted by Zener's theory. A summary is given in Sec. V.

II. THEORY

The theory is based upon the effective-mass approximation. The physical constants and material parameters are summarized in Table I. Unless otherwise noted, we use dimensionless parameters, defined by $\hbar = m_e m_{hs}/(m_e + m_{hs}) = e^2/4\pi\varepsilon_0\varepsilon = e = 1$.

The optical susceptibility is given by[18,21]

$$\chi(\omega) = \frac{1}{i\hbar}\int_0^\infty dt\, e^{+i(\omega+i\epsilon)t}\frac{1}{L}\int_{-L/2}^{+L/2} dZ \int_{-L/2}^{+L/2} dZ' \times \left[\exp\frac{Ht}{i\hbar}\right](\rho=0,Z,Z;\ \rho'=0,Z',Z'), \tag{2}$$

with the electron-hole Hamiltonian

$$\hat{H} = -\frac{1}{2m_\rho}\Delta_\rho - \frac{1}{2m_e}\frac{\partial^2}{\partial z_e^2} - \frac{1}{2m_{hz}}\frac{\partial^2}{\partial z_h^2} + U_e(z_e) + U_h(z_h) + F(z_e - z_h) + \frac{B^2}{8m_\rho}\rho^2 - \frac{1}{\sqrt{\rho^2 + (z_e - z_h)^2}}. \tag{3}$$

The superlattice potentials U_e and U_h describe the modulations of the band edges with the period a and are calculated from the parameters in Table I. The radius of the relative in-plane motion is denoted by ρ and the reduced in-plane mass is $m_\rho = m_e m_{h\rho}/(m_e + m_{h\rho})$. A magnetic field B in growth (z) direction acts as an effective parabolic potential

and leads to Landau quantization of the in-plane motion. We always consider an ideally periodic structure in the limit $L \to \infty$. The photon energy $\hbar\omega$ is defined relative to the fundamental gap. Some prefactors are omitted in the definition of χ, because we are not interested in the absolute numbers.

We first numerically solve Eq. (2) by discretizing the differential operator (3) in real space. To take advantage of the translational symmetry in the growth direction, we introduce center and relative coordinates, generally defined as $Z = c_e z_e + c_h z_h$ and $z = z_e - z_h$ with c_e, c_h real and $c_e + c_h = 1$. Then the Hamiltonian (3) is periodic in the coordinate Z. The commonly used center-of-mass and relative coordinates with $c_e = m_e/(m_e + m_{hz})$ and $c_h = m_{hz}/(m_e + m_{hz})$ are not the first choice for the numerical calculation, because they do not lead to equally spaced z_e and z_h. We use $Z = z_h$ and $z = z_e - z_h$ so that z_e and z_h are equally spaced and are on the same mesh as Z and z.

The exponential of the operator in Eq. (2) is calculated by the equation-of-motion method. We solve the Schrödinger equation for the exciton wave function

$$i\hbar \frac{d}{dt}\Psi = \hat{H}\Psi \tag{4}$$

with the initial condition

$$\Psi(\rho, Z, z, t=0) = \frac{\delta(\rho)}{2\pi\rho}\,\delta(z). \tag{5}$$

Because of the periodicity in Z it is sufficient to consider the interval $Z \in [-a/2, +a/2]$. The optical susceptibility then takes the form

$$\chi(\omega) = \frac{1}{i\hbar}\int_0^\infty dt\, e^{+i(\omega + i\epsilon)t}\,\frac{1}{a}\int_{-a/2}^{+a/2} dZ\, \Psi^* \times (\rho=0, Z, z=0, t=0)\,\Psi(\rho=0, Z, z=0, t). \tag{6}$$

The discretization of the δ function and the radial part of the Laplacian is explained in Ref. 22. The operator of the kinetic energy does not need to be transformed to the center and relative coordinates. Instead, the derivatives can be directly applied to the (Z,z) mesh. To avoid the singularity at the origin, the Coulomb potential is discretized by means of the ground-state method.[22]

In order to model continuum states far above the absorption edge, the domain for the in-plane motion needs to be huge, with a radius typically in the order of 100. The numerical effort and storage can be reduced by means of absorbing boundary conditions. Their usefulness in the calculation of optical spectra has recently been demonstrated by Ahland *et al.*[23] For this purpose, we replace the operator of the kinetic energy by

$$\hat{H}_{\mathrm{kin}\,\rho} = -\frac{1}{\rho}\,\frac{\partial}{\partial\rho}\,\frac{\rho}{2m_\rho \lambda(\rho)}\,\frac{\partial}{\partial\rho}. \tag{7}$$

Inside the region $0 \leqslant \rho \leqslant R_1$ (active layer), λ is equal to unity. For $R_1 < \rho < R_2$ (absorber) it holds that $0 < \arg\lambda < \pi$ and $|\lambda| \to \infty$ as $\rho \to R_2$. The effect of the complex effective mass is twofold: the increase of the real part reduces the wavelength for a fixed energy and the imaginary part leads to the damping of the wave packet. The Hamiltonian is no longer Hermitian and the equation of motion is solved by a combination of leap-frog and Euler scheme for the Schrödinger- and diffusionlike parts of $\hat{H}$. In the present case, a radius of the active region $R_1 = 15$ and an outer radius $R_2 = 20$ gave satisfactory results. The step sizes used for the calculation were $\Delta\rho = 1/8$ and $\Delta z = a/28 \ldots a/14$.

The approximation by Wannier or Kane functions has become a standard method in the treatment of superlattices in electric fields.[6,10,21] The optical spectra calculated with this method show a reasonable agreement with the experiment.[7,8] For a fixed miniband, all Wannier functions can be obtained from one function by $w_n(z) = w_0(z - na)$, where n is the site index. In the following, we will consider only the lowest miniband. In principle, it is possible to take into account a finite number of minibands. In this case, one would observe interaction between different Wannier-Stark ladders and resonant Zener tunneling. However, this expansion is not convergent with respect to the number of minibands and is not suitable to describe nonresonant Zener tunneling.

If we expand Eqs. (2) and (3) into symmetric or antisymmetric Wannier functions,[24,25] carry out the limit $L \to \infty$, and exploit the periodicity with respect to the center coordinate, the optical susceptibility becomes

$$\chi(\omega) = \frac{1}{i\hbar}\int_0^\infty dt\, e^{+i(\omega + i\epsilon)t}\frac{1}{a}\sum_{nn'} \psi_n^* \times \left[\exp\frac{ht}{i\hbar}\right]_{nn'} (\rho=0, \rho'=0)\,\psi_{n'}, \tag{8}$$

where

$$\psi_{n_e - n_h} = \int_{-\infty}^{+\infty} dz\, w_{en_e}(z)\, w_{hn_h}(z) \tag{9}$$

are the overlap integrals between electron and hole Wannier functions and

$$\begin{aligned}\hat{h}_{nn'} = {} & \frac{1}{2m_\rho}\Delta_\rho\,\delta_{nn'} + \int dz\, w_{en}^*(z) \times \left[\frac{1}{2m_e}\frac{d^2}{dz^2} + U_e(z)\right] w_{en'}(z) \\ & + \int dz\, w_{hn'}^*(z)\left[\frac{1}{2m_{hz}}\frac{d^2}{dz^2} + U_h(z)\right] w_{hn}(z) \\ & + F\,a\,n\,\delta_{nn'} + \frac{B^2}{8m_\rho}\rho^2\,\delta_{nn'} \\ & - \int_{-\infty}^{+\infty} dz\,\frac{1}{\sqrt{\rho^2 + z^2}}\sum_{N'}\int_{-\infty}^{+\infty} dZ\, w_{en}^* \times (Z+z)\, w_{e,n'+N'}(Z+z)\, w_h^*(Z)\, w_{hN'}(Z)\end{aligned} \tag{10}$$

are the matrix elements of the Hamiltonian.

For weakly coupled superlattices, the tight-binding approximation gives satisfactory results.[6] In the present case, because of the strong coupling, we took into account coupling between five neighbors. The numerical effort is much smaller than for the solution in real space and it was not necessary to implement absorbing boundary conditions. The domain radius for the numerical calculation was $R=128$.

The upper limit of the time integration (6, 8) was replaced by $5.5/\epsilon$. The convergence was checked with respect to time integration, the discretization in real space, and the boundary conditions. Therefore, the results in the next section can be considered as numerically exact solutions.

III. EXPERIMENT

The measurement was done on a shallow superlattice with sample parameters given in Table I. The sample consists of 35 periods, embedded in various buffer layers in order to ensure a linear behavior of the electric field with the applied voltage. On the front side, a semitransparent Schottky contact was deposited, on the back side, an Ohmic contact was applied and the substrate removed by selective etching to perform the measurements in transmission geometry. The high quality of the Schottky contact allows us to perform measurements in a large field range.

Transmission experiments were carried out at a temperature of 10 K in a standard setup using a halogen lamp. The transmission spectrum was corrected for the spectrum of the lamp and for Fabry-Perot interference caused by multiple reflection inside the sample. This was done using a Fabry-Perot transfer function obtained from the transmission spectrum in the nonabsorptive gap region.

The determination of the internal field is somewhat involved due to field screening effects. We determined the fields by comparison of the experimentally observed position of the Wannier-Stark-ladder (WSL) peaks to theory. In the single-particle picture, the peak positions of one pair of Wannier-Stark ladders are of the form

$$E_n = E_0 + neFd; \quad n = 0, \pm 1, \pm 2, \ldots, \tag{11}$$

where n is the ladder index. This picture breaks down in the low-field limit due to interference with Franz-Keldysh oscillations and the dominance of excitons,[21] as well as in the high-field limit due to the Zener effect and the nonlinear current-voltage characteristics of the Schottky contact and the superlattice itself. For this reason, we used a small intermediate field range to calibrate the internal field.

The used shallow superlattice structure has only one below-barrier electron miniband, Therefore, the assumptions of the Zener theory are nearly fulfilled and the shallow confinement should allow the observation of Zener tunneling already at moderate electric fields. Furthermore, sharp resonances due to anticrossing of Wannier-Stark ladders, which mask the Zener effect, are effectively suppressed.

IV. RESULTS

First, we study the Zener breakdown without the magnetic field. Figure 1 compares calculated and measured absorption spectra for $B=0$ and $F=0,\ldots,60$ kV.

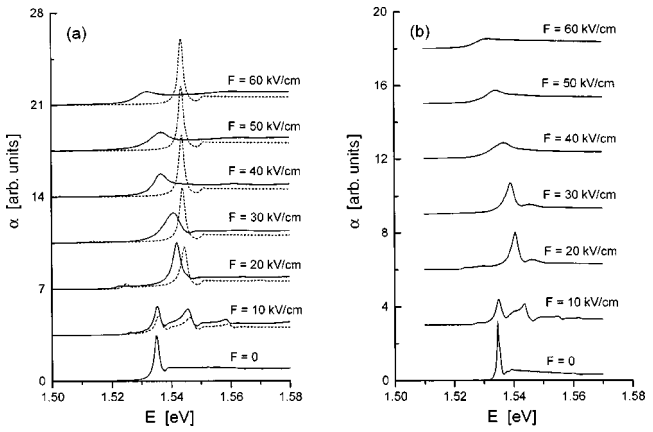

FIG. 1. (a) Absorption spectra for $B=0$ and different values of the electric field $F=0,\ldots,60$ kV/cm. The numerical exact result (solid line) is compared with the approximation by Wannier-Stark levels (dashed line). (b) Experimental absorption spectra for $B=0$ and the same values of F.

Figure 1(a) shows the results of the numerical calculation. The full solution in real space (solid line) is compared with the solution from the one-miniband approximation (dashed line). For $F=0$, the spectrum of the superlattice without field is reproduced. The height of the (2, 2) exciton is very small due to Fano interference with the first subband. There is also a very small feature related to the weakly allowed (1, 3) transition.

For small fields, the typical Wannier-Stark ladder appears. This effect is very pronounced at 10 kV/cm. The transition $n=0$ is located in the middle of the first miniband and transitions with $n \geqslant 0$ show the typical Fano line shape. This effect has been predicted by Whittaker,[6] and was observed by Holfeld *et al.*[7] The one-miniband approximation has a smaller oscillator strength than the numerically exact result, while the peak positions are about the same. The reason is that the Wannier functions of a single miniband are not a complete orthonormal system. This projection reduces the oscillator strength, which is proportional to the exciton wave function at $\rho=z=0$. This effect is generally observed in calculations based upon subband expansions. Furthermore, the oscillator strength of the continuum, relative to the single peaks, is smaller for the approximate solution than for the exact solution.

For $F=20$ kV/cm, both spectra are still very similar. The main difference is the position of the peaks. The main peak of the full solution is shifted to lower energies. This is primarily an effect of the single-particle energies, which depart from the Kane approximation. This behavior is also observed in the optical density of states, which does not take into account Coulomb interaction.[18] The linewidth is slightly increased, in comparison with the approximate solution.

A different behavior of exact and approximate solution is observed for large fields, $F \geqslant 30$ kV/cm. In the one-subband approximation, the line narrows and the spectrum becomes nearly independent of the electric field. The half width at half maximum (HWHM) has narrowed to 1 meV, which is the value of the homogeneous broadening. This is because the

Fano coupling decreases with the field.[7] Eventually, one obtains a spectrum of a two-dimensional semiconductor. In contrast, within exact treatment the linewidth increases with field, because of Zener tunneling. At 30 kV/cm the linewidth (HWHM) is 3 meV. While it is difficult to experimentally decide whether the line broadening is due to Fano interference or Zener tunneling, the theoretical calculations are helpful for a clearer distinction. As the Fano linewidth decreases with field, but the Zener linewidth increases, the turnaround of the linewidth as a function of the electric field can be interpreted as the onset of Zener tunneling. The same can be said for the height of the peaks. The reduction of Fano coupling leads to an increasing maximum, while the Zener effect tends to reduce the amplitude. Thus, a maximum in the height of the absorption signals the beginning of the Zener breakdown.

Figure 1(b) shows the measured absorption spectra for the same electric fields as in Fig. 1(a). Despite the limitations of the two-band model and the uncertainties of the field measurement, the general agreement between theory and experiment is very good. This holds true for the structure of the spectrum, i.e., the number of peaks seen and their relative heights, the position of the peaks and evolution of the linewidth with field. In fact, there is hardly any feature that cannot be explained by the theory. Even very small features, such as a saddle-point exciton on the upper edge of the (1, 1) miniband transition at about 1.56 eV are seen both in experiment and theory. The homogeneous linewidth at $F=0$ is smaller than the value assumed in the numerical calculation. The small line broadening at zero field also demonstrates of a very high quality of the sample. There is no doubt that the experimental data do not support the Kane picture [dashed line in Fig. 1(a)], which does not take into account any Zener tunneling, but confirm the result of a full numerical calculation, including all subbands [solid line in Fig. 1(a)]. Therefore, the experimental spectra provide clear evidence for the Zener breakdown.

Having found a good agreement between theory and experiment for the evolution of the optical absorption with electric field, it is interesting to see whether a quantitative analysis of the linewidth confirms the prediction of Zener's theory. Ideally, the linewidth should be given by Eq. (1). However, there are additional scattering mechanisms, which are not related to the Zener effect and lead to a line broadening already at $F=0$. Hence, we should be able to describe the measured linewidth by the following formula:

$$\mathrm{HWHM}=\frac{e}{2\pi}AF\exp\left(-\frac{B}{F}\right)+C. \tag{12}$$

Figure 2 shows the measured linewidth (open circles) and result of the fit to Eq. (12). The fitting parameters are $A=6.09$ nm, $B=21.8$ kV/cm, and $C=0.632$ meV. The fitted curve reproduces the onset of the Zener breakdown and also the trend for high fields. The oscillations of the line broadening with field result from anticrossing with other Wannier-Stark ladders. This behavior is seen in Fig. 3 of Ref. 18, where the optical density of states is plotted versus field for the same sample. The number of anticrossings is proportional to $1/F$. This effect was also described in a recent publication by Glück, *et al.*,[14] where the tunneling rate is calculated on the basis of an analytically solvable model. The oscillations are rather small in shallow superlattices, because the line broadening is dominated by nonresonant Zener tunneling. In contrast, for strong confinement, almost all tunneling is resonant. This point will be studied in more detail in a subsequent publication. Apart from resonant tunneling, the overall behavior of the linewidth with field should be linear, which is confirmed by experiment. Interestingly, the high-field limit is determined solely by the superlattice period, as seen in formula (1). Therefore, the fitting parameter A should be in the order of the superlattice period, which is the case. Also, the parameter B is close to the theoretical value. With the numerical value of the first miniband gap $\Delta E=33.3$ meV and Eq. (1), this number should be 28.2 kV/cm. The parameter C cannot be predicted, but depends on the sample. Taking into account the approximate character of Eq. (1), the simplifications involved with the effective-mass theory, the disturbances by resonant Zener tunneling, and uncertainties with the interpretation of the linewidth (in experiment, the line shapes tend to be more Gaussian than Lorentzian), the agreement between theory and experiment is excellent.

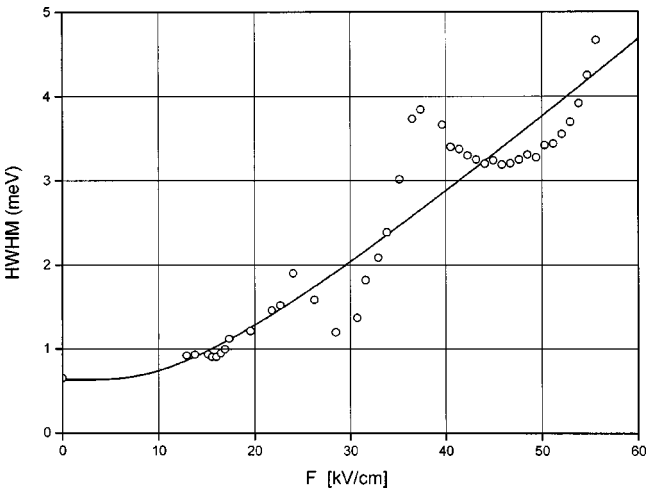

FIG. 2. Linewidth (HWHM) vs electric field F. Open circles: experimental values. Solid line: fit to Eq. (12). Fitting parameters: $A=6.09$ nm, $B=21.8$ kV/cm, $C=0.632$ meV.

Even though the measurements so far provided overwhelming evidence of Zener tunneling, the analysis involved some theoretical background (or bias). A magnetic field perpendicular to the superlattice plane would provide a foolproof way of detecting the Zener breakdown, because the spectrum of the in-plane motion is completely discrete due to Landau quantization and the only source of a continuous spectrum is Zener tunneling. So far, no experimental data are available at the moment. Calculated spectra for a magnetic field of $B=9$ T are shown in Fig. 3 for the same values of F as in Fig. 1. At $F=0$, the spectrum is rather similar to the spectrum of a bulk semiconductor in a magnetic field where different Landau levels appear and excitons of excited Landau levels are changed into Fano resonances.[26] This is because, in the vicinity of the band gap, the optical density of

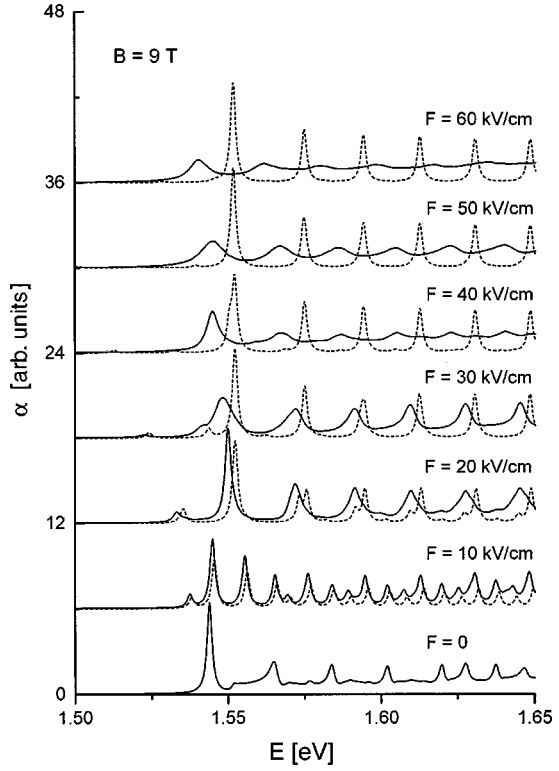

FIG. 3. Absorption spectra for a magnetic field $B=9$ T in growth direction. The other parameters are the same as for Fig. 1(a).

states for a shallow superlattice behaves like the optical density of states of a bulk semiconductor.

For $F>0$, Wannier-Stark quantization takes place in the growth direction. For low fields, $F=10$ kV/cm, the spectrum is entirely discrete and has a complicated structure due to intermixing of Landau and Wannier-Stark quantization. The approximate solution is very similar to the exact solution, and the difference consists mainly in the oscillator strengths of the transition, as observed already for $B=0$.

Starting at $F=20$ kV/cm, approximate and exact solutions behave already differently. With increasing field, the approximate solution changes into the spectrum of a two-dimensional semiconductor in a magnetic field.[27] The linewidth does not change and is entirely determined by the homogeneous broadening. The lines that belong to higher Landau levels show a pronounced level broadening. In contrast, for the lowest Landau level, the difference of the linewidth between exact and approximate solution is small, even smaller than in Fig. 1(a). We address this difference to different exciton binding energies of the Landau levels. Since the exciton energy E_B also provides a barrier for tunneling, the effective field strength is about equal to $F-E_B/ea$. This reduction is in the order of 4 kV/cm and depends on the magnetic field as well as on the Landau level.

At 30 kV/cm, we observe a drastic increase of the linewidth for the lowest Landau level due to Zener tunneling. Another feature can be seen observed for the higher Landau levels. Their peaks show a slightly asymmetric line shape. Besides the removal of the Wannier-Stark states, the Zener tunneling also leads to an increase of the density of states between the Wannier-Stark resonances. The quantum interference of the higher Landau levels with this continuum results in the asymmetric line shapes. This continuum always exists, but its oscillator strength is negligibly small before the Zener breakdown.[28]

For higher fields, the broadening of all peaks increases and the peaks of the excited Landau levels eventually disappear, leaving a small modulation of the spectrum. As the Landau quantization removes the Fano effect of the in-plane motion, the observed broadening is entirely an effect of Zener tunneling in the growth direction.

V. SUMMARY

In this paper we presented calculations of the absorption spectra of a shallow superlattice in an electric field, including Coulomb interaction. The results of the full numerical calculation show a strong influence of Zener tunneling with increasing electric field, which is not observed in the solution based upon the Kane approximation. This comparison also allows us to distinguish between broadening due to Zener tunneling and broadening due to Fano interference.

The experimental spectra confirm the picture in great detail. The Zener effect is observed for the same field range as predicted by theory. The comparison with both the full numerical calculation and the Kane approximation definitely supports the assumption of Zener tunneling.

The measured linewidth as a function of the electric field essentially behaves as predicted by Zener theory. The fitting parameters are in reasonable agreement with the prefactors in Eq. (1), calculated from the sample parameters. The picture is somewhat distorted by oscillations of the linewidth, which are attributed to crossings with other Wannier-Stark ladders.

We also suggest an experimental detection of the Zener effect for a magnetic field applied in the growth direction. For the sample under consideration the theoretical calculations predict a strong line broadening due to Zener tunneling at intermediate electric fields, starting with the higher Landau levels. At high electric fields, the Landau levels should be almost washed out.

ACKNOWLEDGMENT

Wa acknowledge the computing time provided by the John von Neumann Institute for Computing, Forschungszentrum Jülich.

[1] G. H. Wannier, Phys. Rev. **117**, 432 (1960).
[2] J. E. Avron, J. Zak, A. Grossmann, and L. Gunther, J. Math. Phys. **18**, 918 (1977).
[3] L. Esaki and R. Tsu, IBM J. Res. Dev. **61**, 61 (1970).
[4] E. E. Mendez, A. Agulló-Rueda, and J. M. Hong, Phys. Rev. Lett. **60**, 2426 (1988).
[5] P. Voisin, J. Bleuse, C. Bouche, S. Gaillard, C. Alibert, and A. Regrency, Phys. Rev. Lett. **61**, 1639 (1988).

[6] D. M. Whittaker, Europhys. Lett. **31**, 55 (1995).
[7] C. P. Holfeld, F. Löser, M. Sudzius, K. Leo, D. M. Whittaker, and K. Köhler, Phys. Rev. Lett. **81**, 874 (1998).
[8] A. Thränhardt, H.-J. Kolbe, J. Hader, T. Meier, G. Weiser, and S. W. Koch, Appl. Phys. Lett. **73**, 2612 (1998).
[9] K. Leo, P. Haring Bolivar, F. Brüggemann, R. Schwedler, and K. Köhler, Solid State Commun. **84**, 943 (1992).
[10] M. M. Dignam, J. E. Sipe, and J. Shah, Phys. Rev. B **49**, 10 502 (1994).
[11] H. Schneider, H. T. Grahn, K. v. Klitzing, and K. Ploog, Phys. Rev. Lett. **65**, 2720 (1990).
[12] A. Sibille, J. F. Palmier, and F. Laruelle, Phys. Rev. Lett. **80**, 4506 (1998).
[13] M. Helm, W. Hilber, R. De Meester, F. M. Peeters, and A. Wacker, Phys. Rev. Lett. **82**, 3120 (1999).
[14] M. Glück, A. R. Kolovsky, and H. J. Korsch, Phys. Rev. Lett. **83**, 891 (1999).
[15] C. Zener, Proc. R. Soc. London, Ser. A **145**, 523 (1934).
[16] Qian Niu and M. G. Raizen, Phys. Rev. Lett. **80**, 3491 (1998).
[17] B. Rosam, F. Löser, V. G. Lyssenko, K. Leo, S. Glutsch, F. Bechstedt, and K. Köhler, Physica B **272**, 180 (1999).
[18] S. Glutsch and F. Bechstedt, Phys. Rev. B **60**, 16 584 (1999).
[19] T. Yamanaka, K. Wakita, and K. Yokoyama, Appl. Phys. Lett. **65**, 1540 (1994).
[20] W. Bardyszewski, D. Yervik, C. Rolland, and E. Dupont, Phys. Rev. B **60**, 16 563 (1999).
[21] N. Linder, Phys. Rev. B **55**, 13 664 (1997).
[22] S. Glutsch, D. S. Chemla, and F. Bechstedt, Phys. Rev. B **54**, 11 592 (1996).
[23] A. Ahland, D. Schulz, and E. Voges, Phys. Rev. B **60**, R5109 (1999).
[24] W. Kohn, Phys. Rev. **115**, 809 (1959).
[25] S. Glutsch, J. Phys.: Condens. Matter **11**, 5533 (1999).
[26] S. Glutsch, U. Siegner, M.-A. Mycek, and D. S. Chemla, Phys. Rev. B **50**, 17 009 (1994).
[27] C. Stafford, S. Schmitt-Rink, and W. Schäfer, Phys. Rev. B **41**, 10 000 (1991).
[28] M. Ritze, N. J. M. Horing, and R. Enderlein, Phys. Rev. B **47**, 10 437 (1993).
[29] U. Rössler, Solid State Commun. **65**, 1279 (1988).
[30] S. Adachi, *GaAs and Related Materials* (World Scientific, Singapore, 1994).